Microwave-Assisted Preparation of Poly(2-EHA-*co*-ST) Copolymer and Poly(2-EHA-*co*-ST)/MMT Nanocomposite

Trinath Biswal,[1,2] Ramakanta Samal,[3] Prafulla K. Sahoo[1]

[1]*Department of Chemistry, Utkal University, Vani Vihar, Bhubaneswar 751004, India*
[2]*Department of Chemistry, Trident Academy of Technology, Bhubaneswar 751024, India*
[3]*Department of Chemistry, Rajendra College, Bolangir 767002, India*

Received 12 June 2011; accepted 24 September 2011
DOI 10.1002/app.36298
Published online 14 January 2012 in Wiley Online Library (wileyonlinelibrary.com).

ABSTRACT: Copolymerization of 2-ethylhexylacrylate and styrene was performed in presence of benzoyl peroxide as initiator at varying concentrations of the comonomers in a microwave oven. Montmorillonite (MMT) clay was added with a view to prepare nanocomposites, which actually enhanced the water absorption capacity and pressure sensitive adhesive properties. The copolymer and its nanocomposite were characterized by Fourier Transform Infrared, ^{1}H- and ^{13}C-NMR, thermogravimetric-differential thermal analysis (TG-DTA), differential scanning calorimeter, scanning electron microscopy, X-ray diffraction (XRD), and transmission electron microscopy (TEM). The MMT layers were partially exfoliated/intercalated during the polymerization process as evident from the XRD and TEM observations. Their adhesive properties, water absorbancy, and biodegradability in different conditions were studied for their future applications. The monomer reactivity ratios were determined using Finemann–Ross and Kelen–Tüdos method. © 2012 Wiley Periodicals, Inc. J Appl Polym Sci 125: 1467–1475, 2012

Key words: copolymers; microwave; nanocomposites; monomer reactivity ratio

INTRODUCTION

Pressure sensitive adhesives (PSAs) enjoy a wide range of applications[1–3] starting from medical field to self-adhesive floor tiles, flypapers, gloss laminations, disposable diapers, tackifying agents, automotive interiors, etc. Out of these, medical PSAs are typically selected from acrylates, polyisobutylenes, and silicones.[4] Formulations of such adhesives with excipients that act as plasticizer, i.e., enhancers in transdermal delivery systems, often requires the high solubility of acrylates, while maintaining the adhesive properties. There have been several attempts to copolymerize various acrylic and nonacrylic polymers with 2-ethylhexylacrylate (2-EHA).[4,5] There has also been some work on copolymerizing styrene (ST) with various other comonomers.[6–9] Work on the therapeutic use as transdermal drug delivery (TDS) has also been done using 2-EHA and ethyl acetate.[10] Although, the copolymer of 2-EHA and ST has been reported, the synthesis of the nanocomposite with montmorillonite (MMT) by microwave irradiation has not been reported yet. Moreover, this article puts emphasis on the adhesive property study of both the copolymer and the nanocomposite.

The copolymerization of an acrylic monomer, 2-EHA with a vinyl monomer, ST was done, and it exhibited PSA property. Furthermore, an additive MMT was added to the copolymer to prepare a nanocomposite with a view to enhance its water absorbing capacity so that it can be a good system to prepare TDS patches.

We have already worked on the swelling behavior of PEHA/SS[11] nanocomposites and have been successful in preparing superabsorbents and also prepared PBMA/SS/MH,[12] PMMA/MMT,[13] PBA/SS,[14] and PAN/SS[15] nanocomposites by emulsifier free emulsion methods in traditional heating. Recently, we have prepared PAN,[16] PAN[17] nanoparticle by microwave oven under the catalytic effect of two different Co(III) complexes. In extension use of microwave, we have prepared poly(2-EHA-*co*-ST) copolymer and poly(2-EHA-*co*-ST)/MMT nanocomposite and studied its various properties.

The characterizations of the copolymer and the nanocomposite were done and compared with regard to their Fourier Transform Infrared (FTIR), X-ray diffraction (XRD), transmission electron microscopy (TEM), ^{1}H- and ^{13}C-NMR spectra. Their thermal properties were studied using TG-DTA and differential scanning calorimeter (DSC). The adhesive strength was determined along with their water absorbing capacity and biodegradation under

Correspondence to: P. K. Sahoo (psahoochemuu@satyam.net.in).

different conditions. The monomer reactivity ratios were determined from the monomer feed ratios and the copolymer ratios using Finemann–Ross and Kelen–Tüdos method.[18–22]

EXPERIMENTAL

Materials

ST and 2-EHA E-Merck, Germany were made free from inhibitor by washing with 5% NaOH solution followed by 3% H_3PO_4 to neutralize the excess NaOH. The monomers were then washed properly with distilled water, dried over anhydrous $CaCl_2$, and distilled under vacuum. Initiator benzoyl peroxide (BPO), obtained from E-Merck, India, was recrystallized from $CHCl_3$/MeOH mixture. MMT clay with cation exchange capacity of 90 mequiv/100 g was from Himedia India and was used without further purification. All other reagents were used as received.

Preparation of 2-EHA-*co*-ST copolymer

The microwave reactor was reconstructed from a Whirlpool T120 microwave oven. The electromagnetic energy was produced by a magnetron at 2.45 GHz; the power could be adjusted between 0 and 700 W continuously. The temperature of the reaction system was monitored with an IR temperature pickup. With an internal cooling flask, the temperature could be adjusted precisely and independently of the microwave power. The microwave-assisted polymerization, by taking distilled 2-EHA with ST at different proportions, was performed in deionized water via stirring. The comonomers in a reaction vessel were stirred with constant velocity at 500 to 600 rpm in N_2 atmosphere, and then the vessel was heated with 700 W microwave irradiation. After a temperature of 60°C was attained in 8 min, the microwave power was reduced to 40 W to maintain the constant temperature. Then, requisite amount of initiator BPO solution was carefully injected to the reaction mixture. The polymerization was accomplished in 2 h. After the required time interval, the reaction was stopped by adding an excess of dry petroleum ether. The samples so formed were removed, and the conversions were determined gravimetrically. The resulting copolymers were purified by refluxing successfully the samples with $CHCl_3$ and 1,4-dioxane and reprecipitating each time with methanol. The resulting sticky copolymer was dried under vacuum at freezing temperature. Then, it was dried at 40°C in vacuum oven till a constant mass.

Preparation of poly(2-EHA-*co*-ST)/MMT nanocomposite

In microwave-assisted polymerization, the preparation of poly(2-EHA-*co*-ST)/MMT nanocomposite was performed by taking requisite amount of distilled 2-EHA with ST in four-fifth part deionized water via stirring in three-necked reaction vessel. At the same time, desired amount of MMT was dispersed in rest one-fifth part of water at same condition for 2 min with constant stirring. The MMT suspension was added to the reaction vessel containing comonomers and stirred with constant velocity at 500 to 600 rpm in N_2 atmosphere; then, the flask was heated with 700 W microwave irradiation. After 2 min, the temperature of system was attained 60°C, and then the microwave power was reduced to 40 W to maintain constant temperature. The requisite amount of initiator BPO solution was carefully injected to the reaction mixture. The polymerization was accomplished in 2 h. After the required time interval, the reaction was stopped by adding an excess of dry petroleum ether. The resulting poly(2-EHA-*co*-ST)/MMT nanocomposite was purified by refluxing successfully the samples with $CHCl_3$ and 1,4-dioxane and reprecipitating each time with methanol. The resulting sticky poly(2-EHA-*co*-ST)/MMT nanocomposite was dried under vacuum at freezing temperature. Then, it was dried at 40°C in vacuum oven till a constant mass.

Characterization

FTIR of the sample was taken within a Perkin Elmer Paragon 500 FTIR (Boston, MA) spectrophotometer using THF as solvent.

The ^{1}H-NMR and ^{13}C-NMR spectra of the copolymers were recorded at 296 K with a Jeol, GSX 400 with 250 Hz cm^{-1} (for ^{1}H-NMR) (Kansas, Dodge city) and 1100 Hz cm^{-1} (for ^{13}C-NMR) using $CHCl_3$ as the solvent. The ^{1}H-NMR spectra were recorded using a spectral width of 5000 Hz, acquisition time 2 min 29 s, pulse decay of 3.27 s, pulse width 15 s with resolution 0.49 and 32 scans. ^{13}C-NMR was taken at 400 scans, 0.655 min acquisition time, 1.53 resolutions, and spectral width of 22,000 MHz.

XRD monitoring diffraction performed on Philips PW-1847 X-ray crystallographic (Utah, Saltlake city) unit equipped with a Guinier focusing camera CuK_2 radiation. Nanoscale structure and surface morphology of poly (2-EHA-*co*-ST)/MMT nanocomposite were investigated by means of TEM (H-7100 Hitachi Co., Dako, CA), operated at an accelerating voltage of 100 kV.

Thermogravimetric analysis (TGA) of the samples was performed using a Shimadzu DTG-50 (Kyoto, Japan) thermal analyzer. The samples were heated to a temperature of 800°C at the rate of 10°C min^{-1} starting from room temperature (30°C) using dry nitrogen with a flow rate of 50 mL min^{-1}.

DSC was recorded on DuPont 910 DSC (Florida) at a heating rate of 10°C min^{-1} with a sample weight of 1.5 mg.

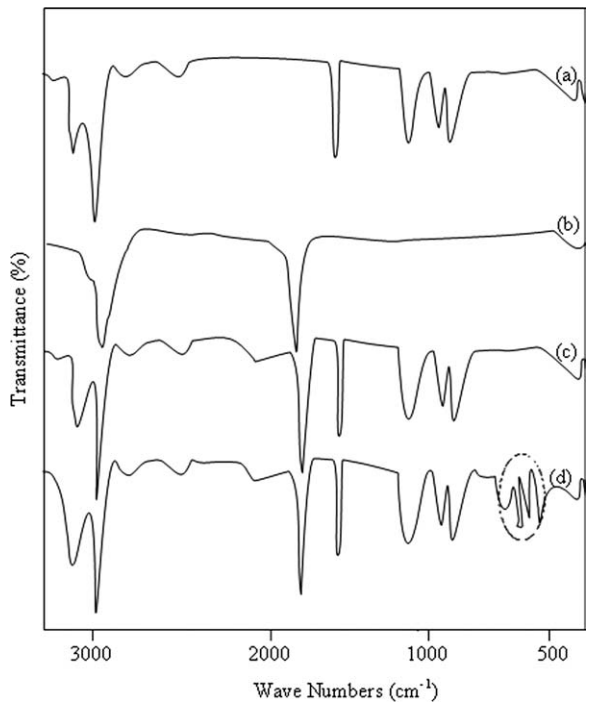

Figure 1 FTIR spectra for (a) polystyrene, (b) poly(2-EHA), (c) poly(2-EHA-*co*-ST) copolymer, and (d) poly(2-EHA-*co*-ST)/MMT nanocomposite.

The surface morphology of the samples was studied by using Jeol, Japan, Model 5200 scanning electron microscope (SEM) at magnification of 1500. A film of the sample ($\sim$ 0.5 mm thick) was first prepared and dried properly under vacuum. Then, a small section was cut, mounted on the stub, coated with gold under a sputter coater, and then studied under the SEM.

The adhesive properties of the copolymers and composites were studied from the adhesive strength measured in terms of peel adhesion. For this purpose, the samples were coated on polyester films to a thickness of 0.5 mm and dried in an oven at 70–80°C for 1 h to ensure complete removal of the solvent. These specimens were subjected to a standard tape adhesion test. The peel adhesion was tested using an Instron type universal testing machine (Minebia Co., Japan model (TCM-1KNB) at a crosshead speed of 300 mm min^{-1}.

The biodegradation of the above samples was studied in sludge water, soil burial, and cultured microorganisms. Samples of known weights were immersed in a standard activated sludge collected from the waste dump areas of the university. The sludge water thus collected was centrifuged, and the supernatant liquid was used for the study. Soil burial is a traditional way to test samples for degradation because of its similarity to actual conditions of waste disposal. For this test, the samples were buried in the soil, collected from paddy fields, at a burrow depth of 1 inch. After the required time intervals, they were recovered from the soil, cleaned with a buffer/ethanol solution and dried in a vacuum oven. The dried samples were weighed to determine the weight loss. Under cultured medium degradation, two types of broth medium were prepared using two different bacteria, *Bacillus cereus* and *Escherichia coli*, using nutrient agar as the base broth medium. The samples were immersed and incubated at 30 $\pm$ 2°C. After regular time intervals, the samples were collected, washed, and the rate of degradation was calculated.

Water absorbency of the samples was studied by immersing the samples ($\sim$ 1 g each) in distilled water at room temperature (30°C) for time periods of 7, 14, 21, 28, and 35 days. The water absorption was determined by weighing the swollen samples after they are allowed to drain on a sieve for 10 min. The percent swelling (mass swelling),[22] % S was calculated using the following equation:

$$\%S = [(m - m_0)/m_0] \times 100$$

where m and m_0 are weights of swollen and dry samples, respectively.

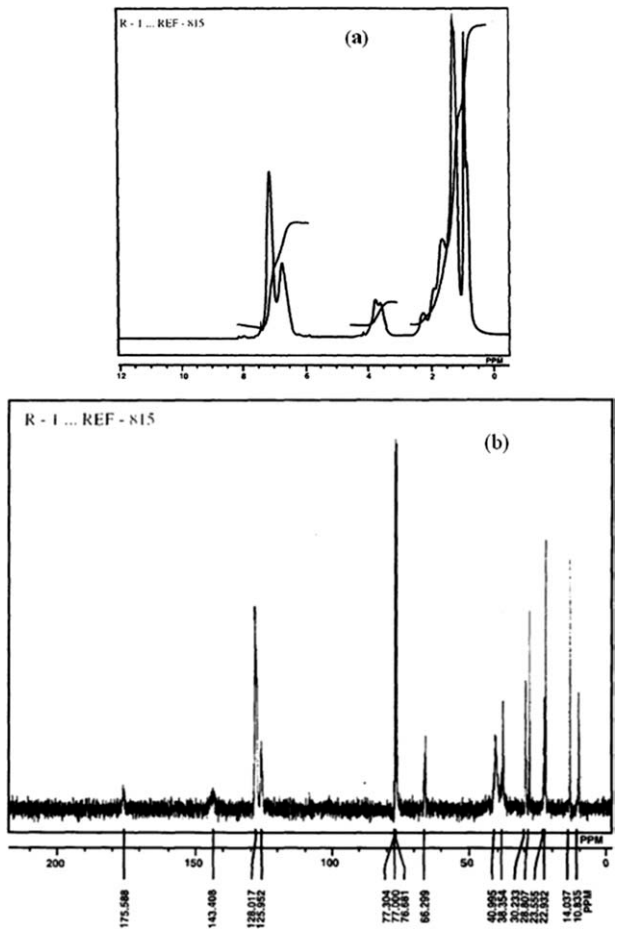

Figure 2 (a) ^{1}H-NMR spectra and (b) ^{13}C-NMR spectra of poly(2-EHA-*co*-ST) copolymer.

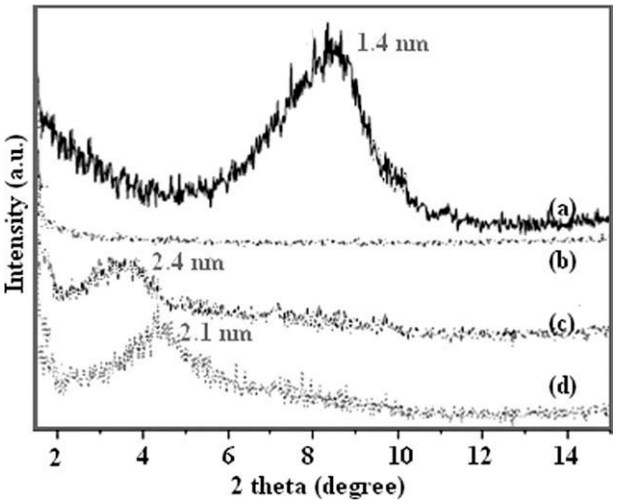

Figure 3 XRD of (a) MMT, (b) poly(2-EHA-*co*-ST)/MMT 5% (w/v), (c) poly(2-EHA-*co*-ST)/MMT 7.5% (w/v), and (d) poly(2-EHA-*co*-ST)/MMT 10% (w/v).

RESULTS AND DISCUSSION

The synthesized copolymer was sticky, transparent, colorless semisolid exhibiting a tacky nature, whereas the composite formed was white, opaque, and tacky.

FTIR

The FTIR spectrum (Fig. 1) of the representative sample exhibited the bonds near 1725 cm^{-1} due to (>C=O)str of the EHA unit, at 3100 cm^{-1} for (C=C)str from aromatic rings, 2930 cm^{-1} for (C-C)str, at 1595 cm^{-1} due to (C-C)str of phenyl groups, and at 700 and 760 cm^{-1} due to (C-H) bending from monosubstituted benzene units of ST, 1150 cm^{-1} for (C-O)str. The results thus obtained showed the possibility of formation of poly(2-EHA-*co*-ST). Further in the FTIR spectrum of the composite, a twin peak at 950 cm^{-1} is characteristic of Si—O—Si bond of silicate, thus confirming the formation of the composite.

NMR

The high-resolution ^{1}H-NMR spectrum of the samples is shown in Figure 2(a). The signal around 1.25–

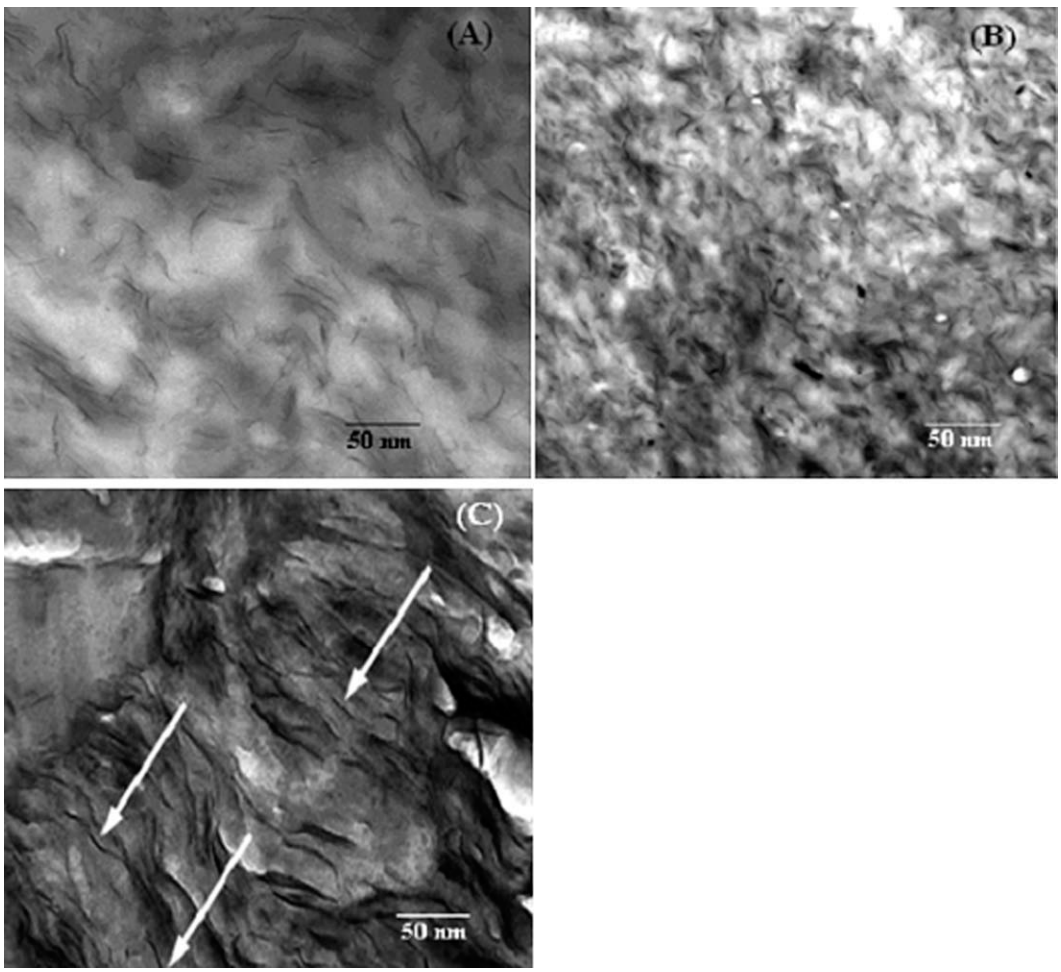

Figure 4 TEM of (a) poly(2-EHA-*co*-ST)/MMT 5% (w/v), (b) poly(2-EHA-*co*-ST)/MMT 7.5% (w/v), and (c) poly(2-EHA-*co*-ST)/MMT 10% (w/v).

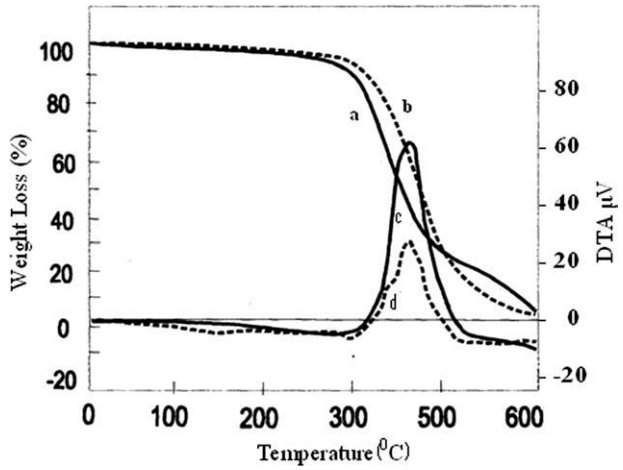

Figure 5 TGA and DTA thermograms of (a) poly(2-EHA-*co*-ST) copolymer and (b) poly(2-EHA-*co*-ST)/MMT (5% w/v) nanocomposite and DTA thermograms of (c) poly(2-EHA-*co*-ST) copolymer and (d) poly(2-EHA-*co*-ST)/MMT (5% w/v) nanocomposite.

2.2 ppm might be due to the -CH_2 protons from ST and EHA molecules. The signal around 3.5–4 ppm is the -OCH_2 from EHA. The aromatic protons from ST show splitting into two peaks around 6.25–6.75 and 6.75–7.5 ppm due to ortho and meta-para protons, respectively. ^{13}C-NMR peak assignments of the copolymer [Fig. 2(b)] are: 22.932–23.555 ppm (-CH_3); 38.35–41.0 ppm (-CH_2- carbons in backbone); 66.299 ppm (-OCH_2-CH-(O)-CH_2-O- carbons); 125.952, 128.017, and 143.408 ppm (aromatic ring); 175.588 ppm (br) (—C=O).

XRD

The systematic arrangement of the silicate layers of MMT in the intercalated/exfoliated nanocomposites have been elucidated by XRD in calculating interlayer spacing with the help of Bragg's equation, the *d*-spacing of MMT has been calculated to be 1.4 nm. Due to the intercalation of poly(2-EHA-*co*-ST) into galleries of silicate of MMT via emulsion polymerization, the *d*-spacing of poly(2-EHA-*co*-ST)/MMT nanocomposites increased with shifting of 2θ to lower values. When the silicate content was $\leq$ 5%, the nanocomposites gave no peak in the XRD plot, which suggests that the layers are fully exfoliated. This XRD pattern of poly(2-EHA-*co*-ST)/MMT nanocomposites as shown in Figure 3(b) indicated the complete disappearance of clay peak, which concluded the better dispersion and exfoliation of silicate layers over poly(2-EHA-*co*-ST) copolymer matrix at lower concentration. With increasing the concentration of MMT % in poly(2-EHA-*co*-ST) copolymer matrix, the exfoliated structure is changed to partial exfoliated and then intercalated as shown in Figure 3(c,d), which was explained in our previous article[13] and is further evident from the corresponding TEM Figure 4.

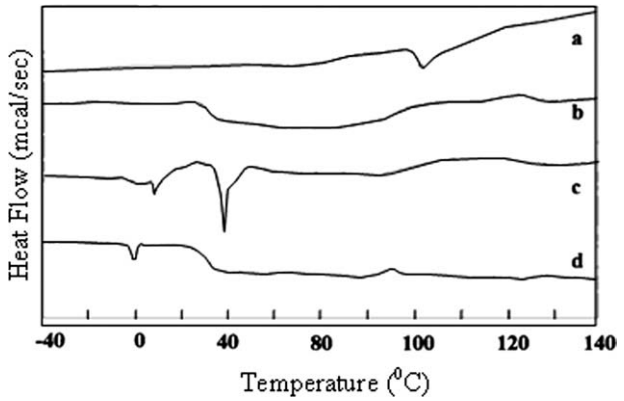

Figure 6 DSC curves of (a) ST, (b) PEHA, (c) poly(2-EHA-*co*-ST), and (d) poly(2-EHA-*co*-ST)/MMT (5% w/v) nanocomposite.

TEM

TEM studies are necessary to verify the extent of exfoliation/intercalation achieved as shown in Figure 4(a–c) for 5, 7.5, and 10 wt % samples. In Figure 4(a–c), it is shown that the MMT layers are well dispersed in the poly(2-EHA-*co*-ST) copolymer matrix. Although the MMT layers still retain their orientation to some degree, the MMT are highly delaminated into some thin lamellas by poly(2-EHA-*co*-ST) with a dimension of about 1–3 nm in thickness. When MMT content $\geq$ 7.5%, the layered structure of the MMT is generally intercalated in the polymer matrix (Fig. 4). But at lower concentration of MMT, i.e., $\leq$ 5%, the silicate layers are partially exfoliated, i.e., destructed their orientation, which are in good agreement with their XRD result. On the basis of the evidence from XRD and TEM, the poly(2-EHA-*co*-ST)/MMT nanocomposites with a partially exfoliated or intercalated structure have been successfully prepared via an *in situ* intercalation process in the neutral aqueous media.

TABLE I
Monomer Compositions in Feed and in Copolymer at 60°C, Solvent THF

	Feed compositions		Copolymer compositions		
Samples	M_1 (EHA)	M_2 (ST)	m_1 (EHA)	m_2 (ST)	Conversion %
1	0.1	0.9	0.214	0.756	12.85
2	0.3	0.7	0.387	0.613	8.66
3	0.5	0.5	0.559	0.441	8.01
4	0.7	0.3	0.704	0.296	7.92
5	0.9	0.1	0.905	0.095	7.53

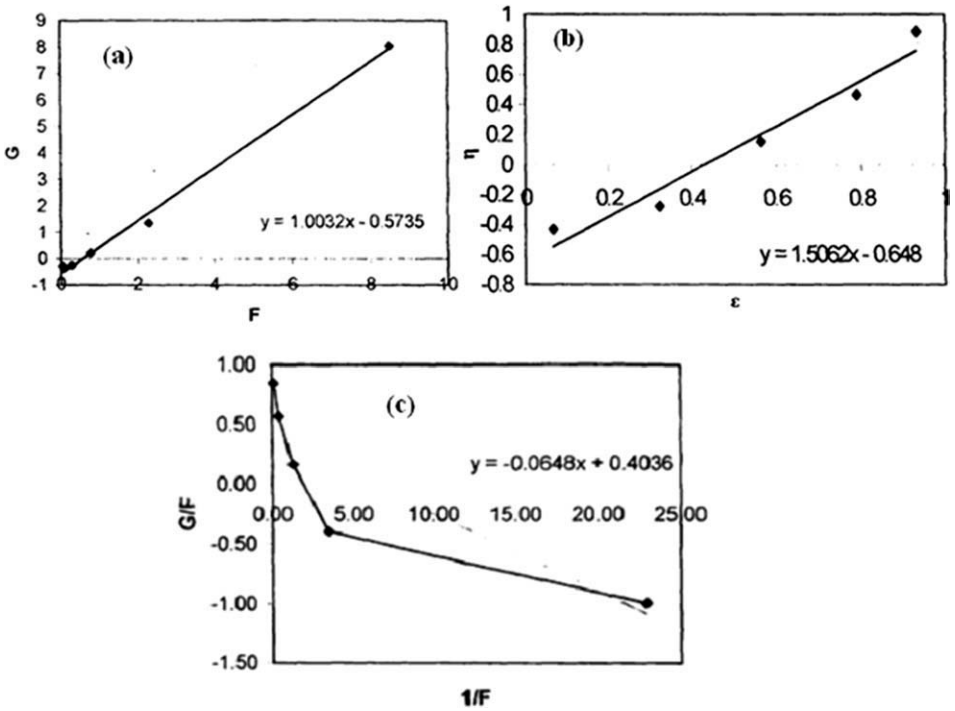

Figure 7 Finemann–Ross plot for poly(2-EHA-*co*-ST), (b) Kelen–Tudos plot for poly(2-EHA-*co*-ST), and (c) Inverted Finemann–Ross plot for poly(2-EHA-*co*-ST).

TGA

The thermal stability of the samples was assessed in terms of integral procedural decomposition temperature (IPDT) value of the copolymers. IPDT values were calculated from the area under the curve and were obtained within experimental errors. In contrast to poly(2-EHA-*co*-ST), the onset of decomposition for poly(2-EHA-*co*-ST)/MMT nanocomposite is shifted toward a higher temperature with increased clay content, indicating an enhancement of the thermal stability on intercalation and addition of inert material. The higher thermal stability of poly (2-EHA-*co*-ST)/MMT nanocomposite suggests that the generated silica-rich char is protecting the polymer from ambient oxygen and reducing the rate of oxidative degradation in the composite materials[23] than that of poly(2-EHA-*co*-ST), which can be attributed to the nanoscale clay layers preventing out-diffusion of the volatile decomposition product. On the other hand, the inorganic part of the nanocomposite film almost did not lose its weight during the heating period. The thermal degradation of the nanocomposite materials have been evaluated by TGA as shown in Figure 5. The weight loss is in the region of 340.2–342.9°C for the copolymer and around 345.0–348.9°C for the composite. This result is further supported by a single distinct exothermic peak in the temperature range of 300–350°C on the DTA curve of the copolymer and 330–370°C of the composite.

DSC

The DSC curves (Fig. 6) reveal the T_g of both the copolymer and the composite and were found to lie in between those of the homopolymers. The T_g of the copolymer (−17°C) was found to be at a lower range than the composite (23°C). Though the reason is not clear, it may be asserted that lower interchain dipole interaction between the copolymer chains

TABLE II
Copolymerization Data for Poly (2-EHA-*co*-ST) Copolymer

Sample	$x = M_1/M_2$	$y = m_1/m_2$	$G = \{x(y-1)\}/y$	$F = x^2/y$	$\eta = G/(\alpha + F)$	$\varepsilon = F/(\alpha + F)$	$1/F$	G/F
1	0.111	0.283	−0.281	0.044	−0.431	0.067	22.93	−0.99
2	0.429	0.631	−0.251	0.292	−0.278	0.323	3.44	−0.40
3	1.000	1.268	0.211	0.789	0.151	0.564	1.27	0.17
4	2.333	2.378	1.352	2.289	0.466	0.790	0.44	0.57
5	9.000	9.526	8.055	8.503	0.884	0.933	0.12	0.85

$\alpha = \sqrt{F_{min}/F_{max}} = 0.61$.

TABLE III
Reactivity Ratios for Poly(2-EHA-*co*-ST) Copolymer

Method	r_1	r_2
Finemann–Ross	1.003	0.574
Kelen	0.882	0.648
Inverted Finemann	0.850	0.404

causes a decrease in the T_g values. Furthermore, it may be suggested that the presence of the hetero silicate particles causes the intermolecular secondary interaction, which makes the composite stiff.

Determination of monomer reactivity ratio

The monomer reactivity ratios for the copolymerization of 2-EHA with ST were determined from the monomer feed ratios and from the copolymer compositions that were calculated from elemental microanalysis. The feed compositions and the copolymer compositions for the copolymerization are given in Table I. Finemann–Ross [Fig. 7(a)], Kelen–Tüdos [Fig. 7(b)], and inverted Finemann–Ross [Fig. 7(c)] methods were used to determine the monomer reactivity ratios as shown in Table II and Figure 7.

From above, the values of r_1 and r_2 were calculated and presented in Table III. Figure 8 shows the plot between the mole fraction of the monomer feed and the copolymer feed. Throughout the reaction, the copolymerization behaviors of the monomer pairs are found to be of the type $r_1 > 1$ and $r_2 < 1$. This is also seen in the reactivity ratio table (Table III). From this, it is clear that the propagation reaction of the type M_{11} and M_{21} is preferred than M_{12} and M_{22}, i.e., the probability of M_1 (2-EHA) entering into the copolymer chain is high, when compared with M_2 (ST). The copolymer formed, therefore will be richer with PEHA. This interesting behavior is confirmed by the predominance of 2-EHA property, i.e., the sticky nature of PEHA is retained throughout the formation of the copolymer.

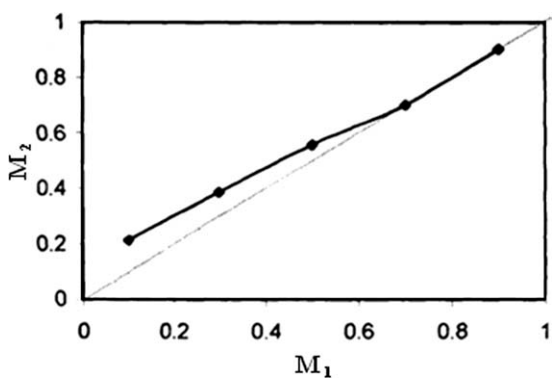

Figure 8 Plot for mole fraction of monomer and copolymer feed in poly(2-EHA-*co*-ST).

TABLE IV
Adhesive Strength of the Copolymers and the Nanocomposites Measured at 30°C with Solvent $CHCl_3$

Sample code	[2-EHA] (mol dm^{-3})	[ST] (mol dm^{-3})	[MMT] (w/v)	Adhesive strength (g cc^{-1})
S_{310}	0.720	0.435	0	148
S_{210}	0.480	0.435	0	507
S_{110}	0.240	0.435	0	1280
S_{120}	0.240	0.870	0	612
S_{130}	0.240	1.305	0	248
S_{111}	0.240	0.435	0.01	1432
S_{112}	0.240	0.435	0.05	1525
S_{113}	0.240	0.435	0.10	1698

S_{abc} = 2-EHA : ST : MMT :: a : b : c.

Peel adhesion

The results of the peel adhesion study of the copolymers and the nanocomposites are tabulated in Table IV. The results of the tape study reveal that with the increase in 2-EHA concentration, the adhesive property decreases. 2-EHA being highly tacky and soft, with the increase in its concentration in the copolymer, the cohesive strength decreases and hence increases the adhesive strength, whereas with the increase in ST concentration in the copolymer, the cohesive strength crosses the optimum level, thus increasing the hardness at the cost of the adhesive strength. Moreover, with the addition of MMT, the adhesive property of the nanocomposite increases rapidly with the increase in silicate concentration.

Biodegradation

From Figure 9, it is clear that the amount of the weight loss increases with time although the rate is very slow (almost negligible). The weight loss in the culture medium was higher, when compared with sludge water or the soil burial tests though the difference is very less. This is obvious as the comonomers, we have taken, are both synthetic and nonbiodegradable. But with the addition of silicate, the biodegradation or the weight loss increases tremendously. This may be due to the higher water penetration resulting in more exposure to microorganism. These new findings will open the door for the composites to be suitable for industrial applications. The biodegradation by soil burial tests of poly(2-EHA-*co*-ST)/MMT (5% w/v) is conformed from SEM Figure 10.

Water absorbency

The percentage swelling of various samples is seen in Figure 11. Though the changes in the rate of water absorption are negligible for the copolymer, with the passing of time, the use of silicate increases

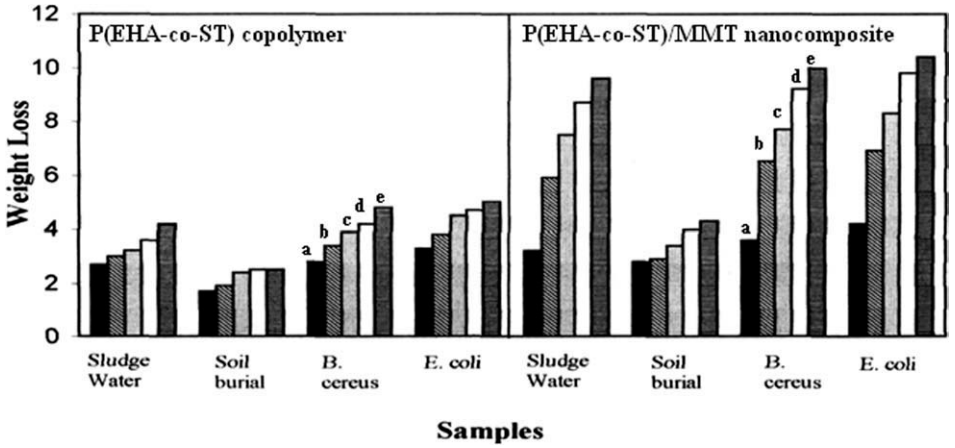

Figure 9 % weight loss due to biodegradation of the samples in different conditions for time periods of (a) 7 days, (b) 14 days, (c) 21 days, (d) 28 days, and (e) 35 days.

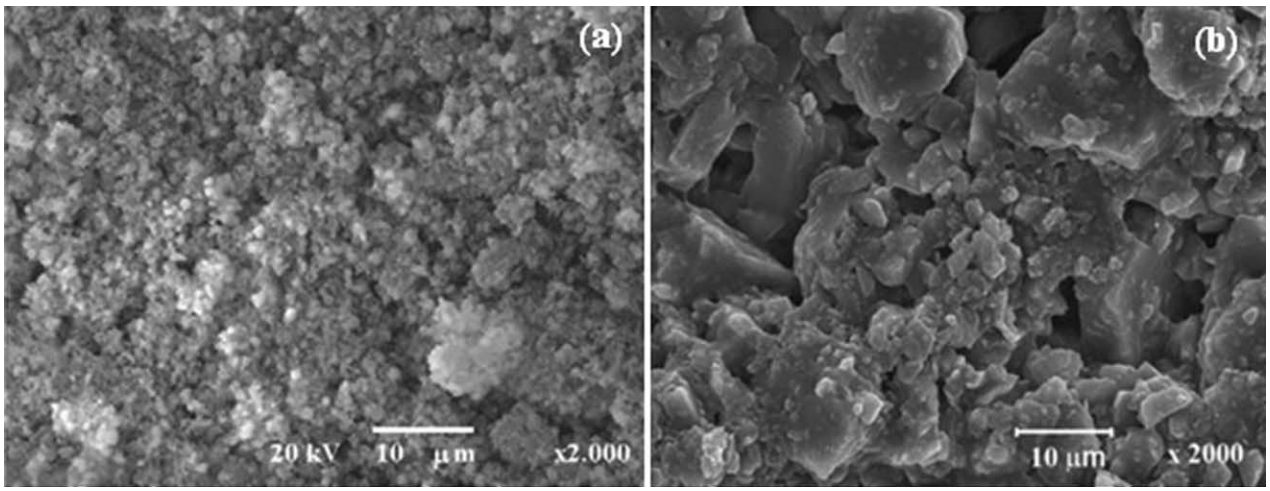

Figure 10 SEM figure of poly(2-EHA-*co*-ST)/MMT (5% w/v) nanocomposite (a) before and (b) biodegradation after 28 days.

the water uptake capacity nearly 100 times due to the porous nature of the MMT clay particles. With excess of MMT, the water absorption decreases due to the increase in the Si-O-Si linkage in the polymer matrix making it dense and less porous.

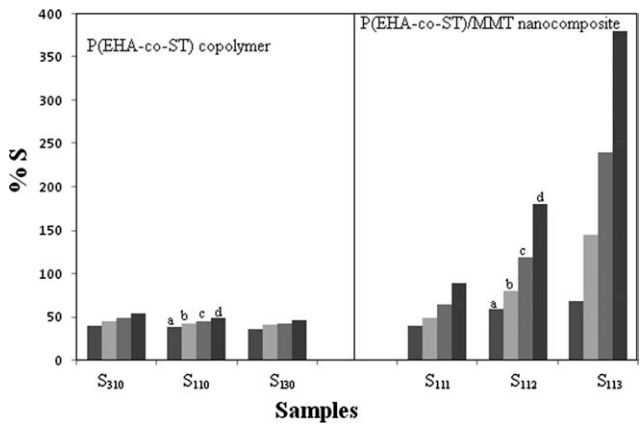

Figure 11 % swelling of the samples in different condition for time periods of (a) 7 days, (b) 14 days, (c) 21 days, and (d) 28 days.

CONCLUSION

In this study, poly(2-EHA-*co*-ST) copolymer and its MMT nanocomposite poly(2-EHA-*co*-ST)/MMT were synthesized. Their characterization was done along with the study of some of their properties like adhesive strength, water absorption, and biodegradation. On comparison of their properties, the composite showed better water absorbency and biodegradation, although there was a fall in the adhesive strength. Studies based on the determination of the monomer reactivity ratios of the copolymer by different methods revealed an interesting phenomenon that the probability of acrylic monomer 2-EHA entering into the copolymer chains high, when compared with the vinyl monomer, ST, making the copolymer richer with PEHA. The synthesis of poly(2-EHA-*co*-ST)

copolymer and its corresponding composites with MMT resulted in materials with distinct properties that have tremendous industrial applications. The use of the additive increases the water uptake capacity of the composite, making it a good candidate for the preparation of adhesive patches for use in the medical field. But, the study of its safety in medical uses is beyond the scope of this article and is open for future research. It showed no irritation, swelling, or maceration of the skin. Hence, its medical application may further be explored.

References

1. Satas, D. Handbook of Pressure Sensitive Adhesive Technology, 2nd ed.; Van Nostrand Reinhold: New York, 1989.
2. Johnston, J. Encyclopedia of Polymer Science and Engineering, Vol. 93; New York: Wiley, 1985.
3. Obori, H.; Takenaga, M. J Appl Polym Sci 1999, 74, 264.
4. Li, X.; Berner, B. J Polym Sci Part A: Polym Chem 1997, 35, 3571.
5. Bhabhe, M. D.; Galvankar, P. S.; Desai, V. M.; Athawale, V. D. J Appl Polym Sci 1995, 56, 485.
6. Sanghvi, P. G.; Pokhriyal, N. K.; Devi, S. Polym Int 2002, 54, 721.
7. McManus, N. T.; Penlidis, A.; Dube, M. A. Polymer 2002, 43, 1607.
8. Wang, Y.; Feng, L.; Pan, C. J Appl Polym Sci 1999, 74, 1502.
9. Stergion, G.; Dousikos, P.; Pitsikalis, M. Eur Polym J 2002, 38, 1963.
10. Manoo, S.; Mimematsa, H.; Kawaguchi, T. Polym J 2000, 32, 171.
11. Rana, P. K.; Swain, S. K.; Sahoo, P. K. J Appl Polym Sci 2004, 93, 1007.
12. Samal, R.; Rana, P. K.; Mishra, G. P.; Sahoo, P. K. Polym Comp 2008, 29, 173.
13. Sahoo, P. K.; Samal, R. Polym Degrad Stab 2007, 92, 1700.
14. Sahoo, P. K.; Samal, R.; Swain, S. K.; Rana, P. K. Eur Polym J 2008, 44, 3522.
15. Samal, R.; Sahoo, P. K. Indian J Chem Tech 2010, 17, 139.
16. Biswal, T.; Samal, R.; Sahoo, P. K. J Appl Polym Sci 2010, 117, 1837.
17. Biswal, T.; Samal, R.; Sahoo, P. K. Nanotech Sci Appl 2010, 3, 77.
18. Naguib, H. F.; Aly, R. O.; Sabaa, M. W.; Mokhtar, S. M. Polym Test 2003, 22, 825.
19. Sundarrajan, S.; Ganesh, K.; Srinivasan, K. S. V. Polymer 2003, 44, 61.
20. Mormann, W.; Ferbitz, J. Eur Polym J 2003, 39, 489.
21. Jone Selvamalar, C. S.; Krithiga, T.; Penlidis, A.; Nanjundan, S. React Funct Polym 2003, 56, 89.
22. Karadag, E.; Saraydin, D. Turk J Chem 2002, 26, 863.
23. Christopher, M. L.; Preston, G. A.; Jefferson, L. H.; Robert, A. S.; Zenka, M. Polym Degrad Stab 2004, 84, 533.